Cross-sectional: MATHEMATICAL MODELING IN POWER ENGINEERING AND INFORMATION TECHNOLOGIES

MODELING OF THERMAL PROCESS PARAMETERS IN THE IONOSPHERE DURING THE DECLINE PHASE OF SOLAR ACTIVITY CYCLE

Vyacheslav Kolodyazhnyi, Mykhaylo Lyashenko

Institute of Ionosphere of the National Academy of Sciences of Ukraine and the Ministry of Education and Science of Ukraine, Kyrpychova str. 16, 61001, Kharkiv, Ukraine; e-mail: Vyacheslav.Kolodyazhnyi@infiz.khpi.edu.ua, M.Lyashenko@nas.gov.ua

Abstract: Simulation of spatial-temporal variations of parameters of thermal processes in ionospheric plasma during the decline phase of solar activity cycle according to the Kharkiv incoherent scatter (IS) radar of is performed. For typical geophysical periods, the diurnal and altitude dependences of the energy supplied to the electron gas and the heat flux density transferred by electrons from the plasmasphere to the ionosphere are constructed. The analysis of spatial and temporal variations of parameters of thermal processes in the ionosphere is given. The obtained calculation results are used for further development of the CERIM IION regional model of ionosphere.

Keywords: *ionosphere, modeling, incoherent scattering, parameters of thermal processes.*

1. Introduction

As is known, at the altitudes of the F2 region of the ionosphere and above, the processes of plasma and energy transfer become more significant than the photochemical processes of formation and disappearance of charged particles. Dynamic and thermal processes play an important role in the formation of the altitude profile of the electron concentration in general, in particular in the F2 region of the ionosphere. Thus, observation, analysis and modeling of variations in the parameters of physical processes in geospace plasma are currently important and relevant tasks of modern geophysics, as they expand our knowledge of the behavior of the parameters of the Earth's atmosphere, ionosphere and magnetosphere.

A large number of publications have been devoted to the study of variations in ionospheric plasma parameters in different heliogeophysical conditions [see, for example, 1–4]. Particular attention is paid to the study of the effects of rare and unique events in the geospace – the strongest geomagnetic storms, solar eclipses and others. However, the study and analysis of the behavior of ionospheric plasma in quiet conditions is no less relevant, because all perturbations unfold against this background.

At present time the Kharkiv IS radar is the only reliable and most informative data source of the geospace plasma parameters in the mid-latitude of Central Europe [5]. The parameters of dynamic and thermal processes in the ionosphere can be calculated with the involvement of experimental IS radar data. The obtained results of calculations are useful for further development of the regional model of the ionosphere CERIM IION [6, 7], which was created at the Institute of the Ionosphere.

The aim of the work is to simulate the spatial-temporal variations of the parameters of thermal processes in the ionospheric plasma during the equinoxes and solstices in 2017–2019 using experimental data of the IS radar in Kharkiv. An empirical model of the atmosphere NRLMSISE-00 was used to calculate the parameters of the neutral atmosphere [8].

2. Observation means

Kharkiv incoherent scatter radar. To study the effects in the ionosphere, the radar of the Institute of Ionosphere of the NAS and MES of Ukraine was used. It is located 50 km from Kharkiv and is the only, most informative source of information on parameters and processes characterizing the behavior of geospace plasma in the European middle latitudes [9]. Radar coordinates: 49.6° N, 36.3° E; geomagnetic: $\Phi = 45.7°$, $\Lambda = 117.8°$; the inclination of the geomagnetic field is 66.4°, the McIlvain parameter $L \approx 1.9$.

The radar is equipped with an zenith two-mirror parabolic antenna with a diameter of 100 m. The operating frequency of the radar is 158 MHz. The effective area of the antenna is about 3700 m^2, the gain of the antenna is about 104, and the width of the main petal of the pattern is about 1°. The pulse power of the radio signal is 2–4 MW. The frequency of transmission of radio pulses is 24.4 Hz. The noise temperature of the radio-receiving device is 120 K, and the bandwidth of the path, which is determined by the low-pass filters, is 5.5–9.5 kHz. The effective noise temperature of the system is 470–980 K.

Digital ionosonde. The digital ionosonde is used for general control of the ionosphere and calibration of the normalized altitude profile of the electron concentration at its maximum (determined by the IS method). The main parameters of the ionosonde: pulse power – 15 kW, duration of radio pulses – 100 μs, frequency range in the mode of vertical sounding 1–20 MHz, receiver sensitivity – 15 μV. Receiving and transmitting antennas – rhombic with vertical

radiation, arranged orthogonally. The error in determining the critical frequency of the layer F2 is not more than 0.05 MHz.

3. Space weather condition

Experimental studies of ionospheric plasma parameters were performed for four characteristic geophysical periods – summer and winter solstice, as well as vernal and autumn equinoxes in quiet geomagnetic conditions in the phase of decline/minimum of the 24th cycle of solar activity. Table 1 presents the dates selected for a detailed analysis of variations in ionosphere parameters and provides information on the state of space weather. In table 1, the indices indicate: $F_{10.7}$ – flux of solar radio radiation at a wavelength of 10.7 cm; A_p – is the total planetary index of geomagnetic activity; K_p – is the value of the planetary index of the magnetic field.

Table 1

Parameters of the space weather condition for the selected dates

Date	$F_{10.7}$	A_p	K_p
Vernal equinox			
23.03.2017	72	11	4 4 2 2 1 2 1 1
29.03.2018	69	4	0 0 1 2 1 2 1 1
21.03.2019	80	2	0 1 1 1 1 0 0 0
Summer solstice			
22.06.2017	74	6	3 2 1 1 1 1 3 2
21.06.2018	82	3	1 1 1 1 1 0 1 0
20.06.2019	68	7	1 2 3 2 1 1 2 2
Autumn equinox			
06.09.2017	133	11	2 2 2 3 3 2 0 4
19.09.2018	68	4	1 3 2 1 0 1 0 0
19.09.2019	67	4	1 1 1 1 1 1 1 1
Winter solstice			
25.12.2017	76	10	3 1 2 3 1 2 3 2
19.12.2018	70	6	1 1 1 2 1 2 1 2
17.12.2019	71	2	0 0 1 1 0 0 0 0

Table 1 shows that almost all periods considered were characterized by quiet geomagnetic conditions and low solar activity. The values of the index $F_{10.7}$ varied in the range from 67 to 82 units. However, on September 6, 2017, there was a slight disturbance of the space weather condition (the value of the index $F_{10.7}$ was 133 units). This is due to the increase in the total area of sunspots and the number of flashes in the active areas.

4. Initial theoretical relations

In this paper, we simulate the parameters of thermal processes in the ionosphere – the energy supplied to the electrons Q/N and the heat flux density Π_T, which is transferred by electrons from the plasmasphere to the ionosphere.

Energy supply to electronic gas. The thermal energy source of charged particles are photons of solar ionizing radiation. The nature of the heating of thermal electrons by photoelectrons differs significantly in the lower ($z \leq$ 250 km) and upper (z>250 km) ionosphere. In regions D and E of the ionosphere, photoelectrons are thermalized mainly at the site of their formation due to the relatively short free path length. This heating of the electron gas is called local. In the upper ionosphere, the frequency of electron collisions with neutrals becomes lower than with ions, and the main mechanisms of electron gas cooling are heat loss during electron collisions with ions, excitation of the fine structure of oxygen atoms, and thermal conductivity of the electron gas. In this case, the transfer of photoelectrons can be neglected, and the associated heating of the electron gas is called non-local.

Consider the altitude range of 210–450 km. At altitudes $z \leq 350$ km, the thermal conductivity of the electron gas can be neglected and the equation of energy balance of electrons in the stationary case has the form [10]

$$\begin{aligned} Q &= L_{ei} + L_e, \\ L_{ei} &= 8\cdot 10^{-32} N^2 (T_e - T_i) T_e^{-3/2}, \\ L_e &= 6.4\cdot 10^{-37} NN(\mathrm{O})(T_e - T_i) T_n^{-1}, \end{aligned} \tag{1}$$

where Q – is the energy transferred to thermal electrons in Coulomb collisions with photoelectrons; L_{ei} – energy loss in electron-ion collisions; L_e – energy loss on the excitation of the fine structure of oxygen atoms; N – the concentration of electrons in the ionosphere; $N(\mathrm{O})$ – concentration of oxygen atoms; T_e – the temperature of electrons; T_i – the temperature of ions; T_n – the temperature of the neutrals.

The electron concentration N, the electron temperature T_e and the ion temperature T_i were obtained experimentally using the IS radar in Kharkiv.

The temperature of the neutrals T_n and the concentration of N(O) are calculated according to the model NRLMSISE-00 [8].

The flux of heat transferred by electrons. The flux of heat from the plasmasphere to the ionosphere plays an important role in the heat balance of the electron gas. The accumulation of heat in the plasmasphere occurs due to the heating of thermal electrons fluxing from the place of its formation into the outer ionosphere. Some electrons lose their energy during Coulomb collisions with thermal electrons and ions. The rest of the electrons enter the magnetic field tube and are heated in it by repeated reflections from the ends of the magnetic tube. Thus, heat accumulates in the plasmasphere, which is then transferred to the ionosphere due to the high thermal conductivity of the electron gas.

The heat flux can be determined from the kinetic equation taking into account the transfer of thermal electrons. The vertical component of the heat flux coming from the plasmasphere is calculated by expression [10]

$$\Pi_T = -\kappa_e \sin^2 I \frac{\partial T_e}{\partial z} \tag{2}$$

where $\kappa_e = 2.08 \cdot k^2 N T_e / m\nu_{ei}$ – the longitudinal component of the thermal conductivity tensor of the electron gas; k – the Boltzmann constant; m – the mass of the electron; I – inclination of the geomagnetic field; z – height.

The frequency of collisions of electrons with O^+ ions to calculate the longitudinal component of the thermal conductivity tensor can be found using the expression

$$\nu_{ei} \approx 5.5 \cdot 10^{-6} N T_e \ln (2.2 \cdot 10^4 T_e N^{-1/3}). \tag{3}$$

5. The results of thermal process parameter modeling under quiet conditions

To calculate the parameters of thermal processes in the geospace plasma, we used experimental data (electron concentration in the ionosphere N, electron temperature T_e, ion temperature T_i), which were obtained on the Kharkiv IS radar during the equinoxes and solstices in 2017–2019. Consider in more detail the spatial-temporal dependences of the thermal process parameters.

The amount of energy supplied to the electrons. The main characteristic of diurnal variations of Q/N is that at night, energy is not supplied to the electrons, and the values of Q/N at this time are close to zero. The increase in the value of Q/N begins at sunrise, and decreases to the background night values – after sunrise. Maximum daily values of Q/N occur in the altitude range of 210–250 km, then with increasing altitude, the value of Q/N decreases.

Vernal and autumn equinoxes. In Fig. 1*a* and Fig. 1*b* presents the diurnal variations in the amount of energy supplied to the electrons for the periods of the vernal and autumn equinoxes in 2017–2019, respectively. For the period of the vernal equinox, these Q/N variations are similar. Maximum Q/N values are observed at an altitude of 210 km and are approximately $27 \cdot 10^{-22}$ J s^{-1} at noon. At an altitude of 350 km $Q/N \approx 1.7 \cdot 10^{-22}$ J s^{-1}. For the period of the autumn equinox we have similar values, however, there is a difference – the values of Q/N for 2017 are many times higher than in 2018 and 2019. One of the reasons for this behavior of Q/N is the disturbed state of the ionosphere.

Summer and winter solstices. In Fig. 1*c* and Fig. 1*d* presents the diurnal variations in the amount of energy supplied to the electrons for the periods of summer and winter solstice in 2017–2019, respectively.

As can be seen from Fig. 1*c*, Q/N values in summer are slightly lower compared to Q/N values during the equinoxes at altitudes of 210–250 km. Thus, the daily values of Q/N at an altitude of 210 km did not exceed $20 \cdot 10^{-22}$ J s^{-1}, and at altitude of 250 km – $Q/N \approx 9 \cdot 10^{-22}$ J s^{-1}. In the altitude range of 300–350 km, Q/N values ranged from $3.7 \cdot 10^{-22}$ J s^{-1} to $2 \cdot 10^{-22}$ J s^{-1}. For the period of the winter solstice Fig. 1*d*, a narrower form of diurnal variations of Q/N was observed in comparison with the forms of diurnal variations in the periods of the equinox and summer solstice, but the maximum value of Q/N in winter was not inferior to the summer values and in the periods of the equinoxes. At altitudes of 210, 250, 300 and 350 km, the value of $Q/N \approx 25 \cdot 10^{-22}$, $7.5 \cdot 10^{-22}$, $3.5 \cdot 10^{-22}$ and $1.25 \cdot 10^{-22}$ J s^{-1}, respectively.

Altitude profiles Q/N are presented in Fig. 2. At night, the value of Q/N is close to zero over the entire range of altitudes. During the day, the maximum values of Q/N occur in the altitude range of 200–300 km, and then with increasing altitude, the value of Q/N decreases to almost zero.

The results obtained in this study are in good agreement with the results obtained earlier in [1–4]. In general, it can be concluded that the extremal values of Q/N strongly depend on the phase of the solar activity cycle, the season, and the space weather state.

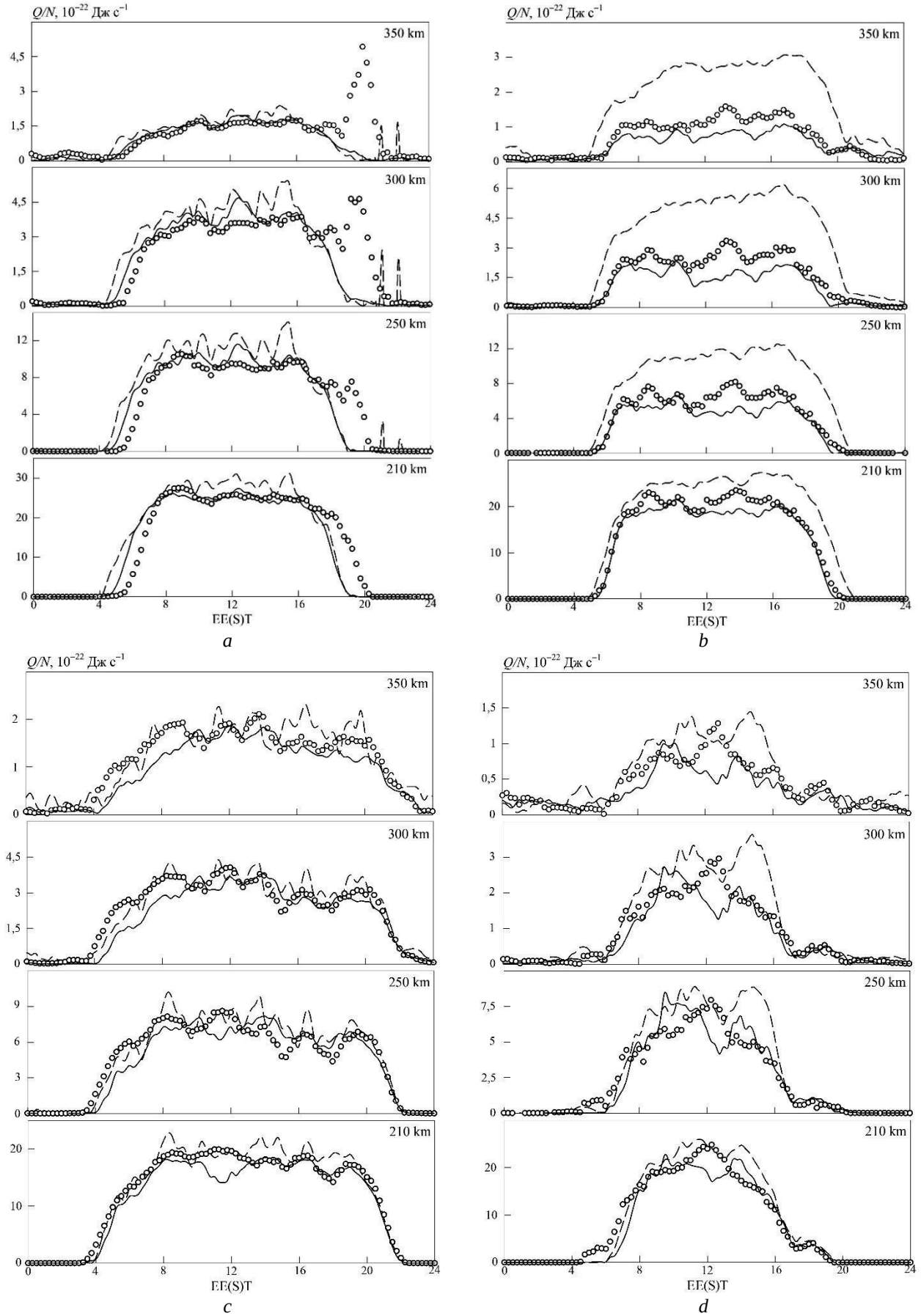

Fig. 1. Diurnal variations in the amount of energy supplied to the electrons *Q/N* in the periods: vernal (*a*) and autumn (*b*) equinoxes; summer (*c*) and winter (*d*) solstice during 2017–2019. Here and further, on the graphs the periods are indicated: dotted line – 2017, circles – 2018, solid line – 2019.

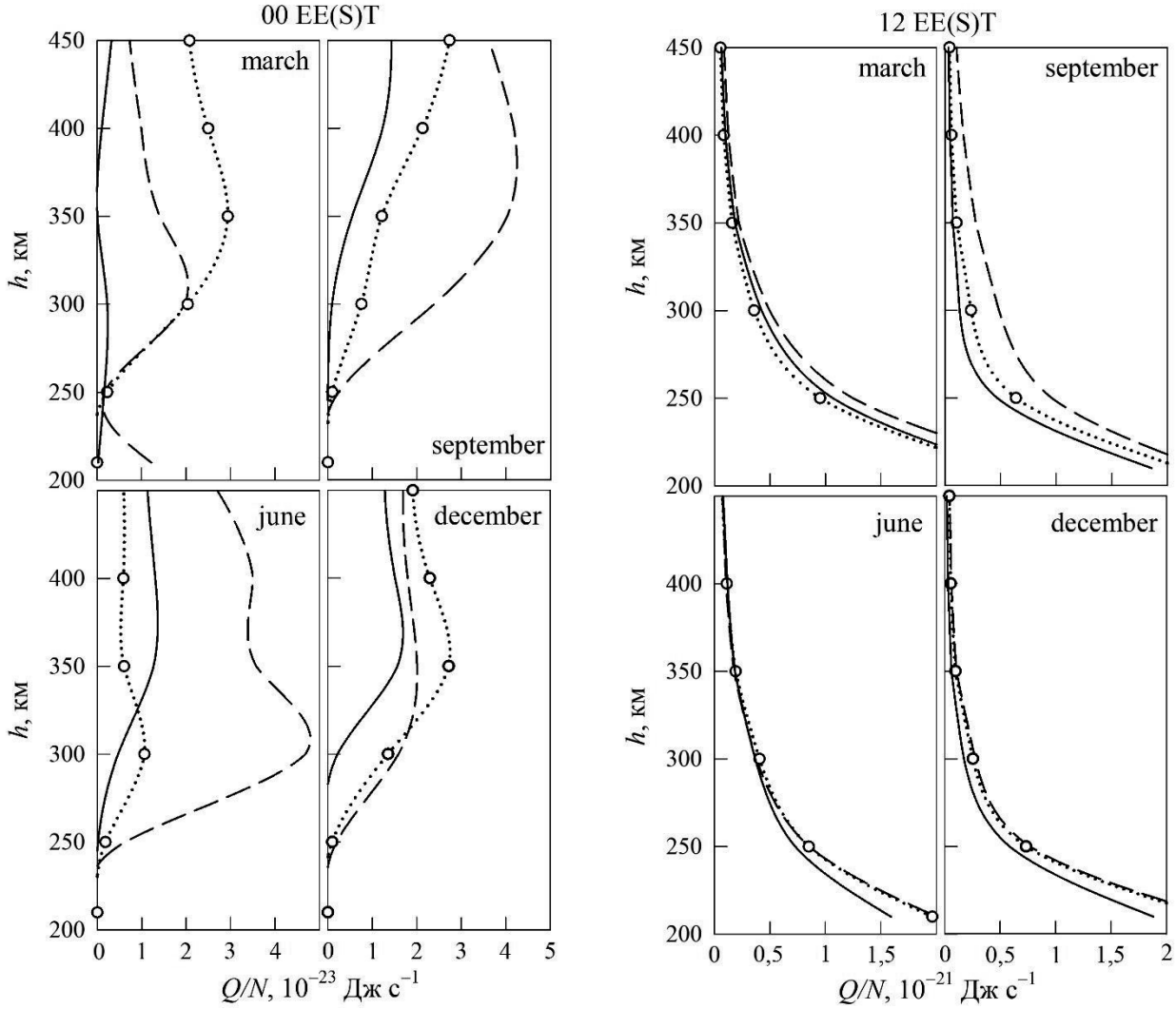

Fig. 2. Altitude profiles of the amount of energy supplied to the electrons *Q/N* in the typical geophysical periods during 2017–2019 for 00 (left panel) and 12 EE(S)T (right panel)

Heat flux density. The main features of the diurnal variations of Π_T are the practical absence of flux at night and the maximum values (by modulus) in the morning and evening.

Vernal and autumn equinoxes. In Fig. 3*a* and Fig. 3*b* shows the diurnal variations in the heat flux transferred by electrons from the plasmasphere to the ionosphere during the vernal and autumn equinoxes in 2017–2019. As can be seen from the Figures, the diurnal variations in Π_T are quantitatively and qualitatively similar. The behavior of Π_T in the vernal and autumn of 2017 is influenced by the state of space weather. In the considered periods of March 23, 2017 and September 6, 2017, the effects of moderate magnetic storms were noticeable in the variations of Π_T (maximum values of K_p index were equal to 4). The main effect of disturbed conditions is an increase in the value of Π_T and an increase in the downward flux of heat into the Earth's ionosphere.

Winter and summer solstice. In Fig. 3*c* and Fig. 3*d* shows the diurnal variations of Π_T in the periods of summer and winter solstice in 2017–2019 at fixed altitudes. The form of diurnal variations during the solstice periods is similar to the forms of time dependences obtained during the vernal and autumn equinoxes. The value of Π_T in summer is about 2 times less than in winter.

As well as for *Q/N*, the magnitude of the heat flux density depends on the level of solar activity and the state of space weather. As can be seen from the figures, even a small perturbation can lead to significant quantitative and qualitative changes in the diurnal variations in Π_T.

In Fig. 4, presents model height profiles of Π_T for noon and midnight. As can be seen from the Figure, at night in the entire altitude range there are quite small values of Π_T compared to daytime. At noon, in the range of altitudes of 300–400 km, the maximum values of the heat flux density, which is transferred by electrons from the plasmasphere to the ionosphere, are observed.

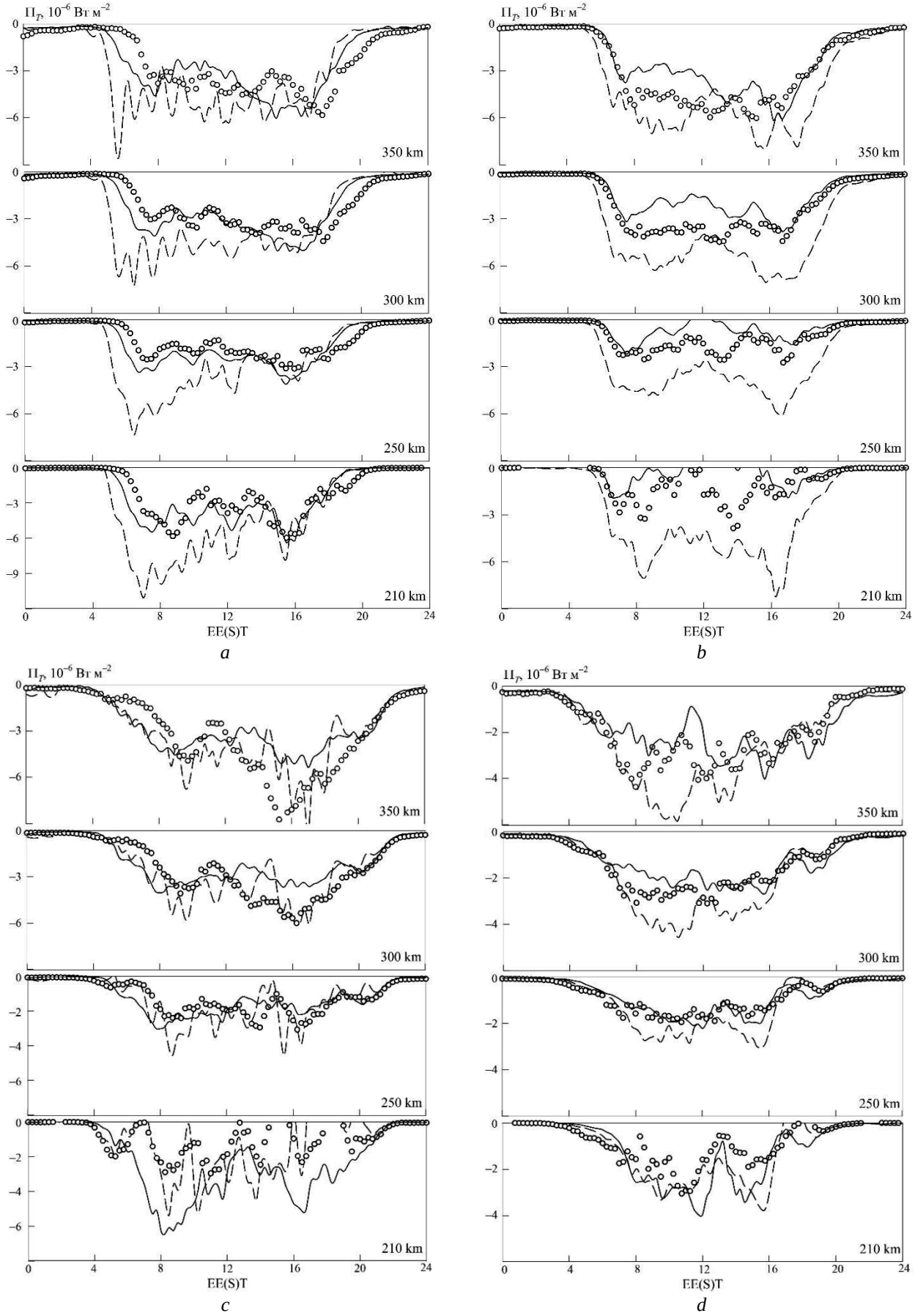

Fig. 3. Diurnal variations in the heat flux density of Π_T, which is transferred by electrons from the plasmasphere to the ionosphere in the periods: vernal (*a*) and autumn (*b*) equinoxes; summer (*c*) and winter (*d*) solstice during 2017–2019

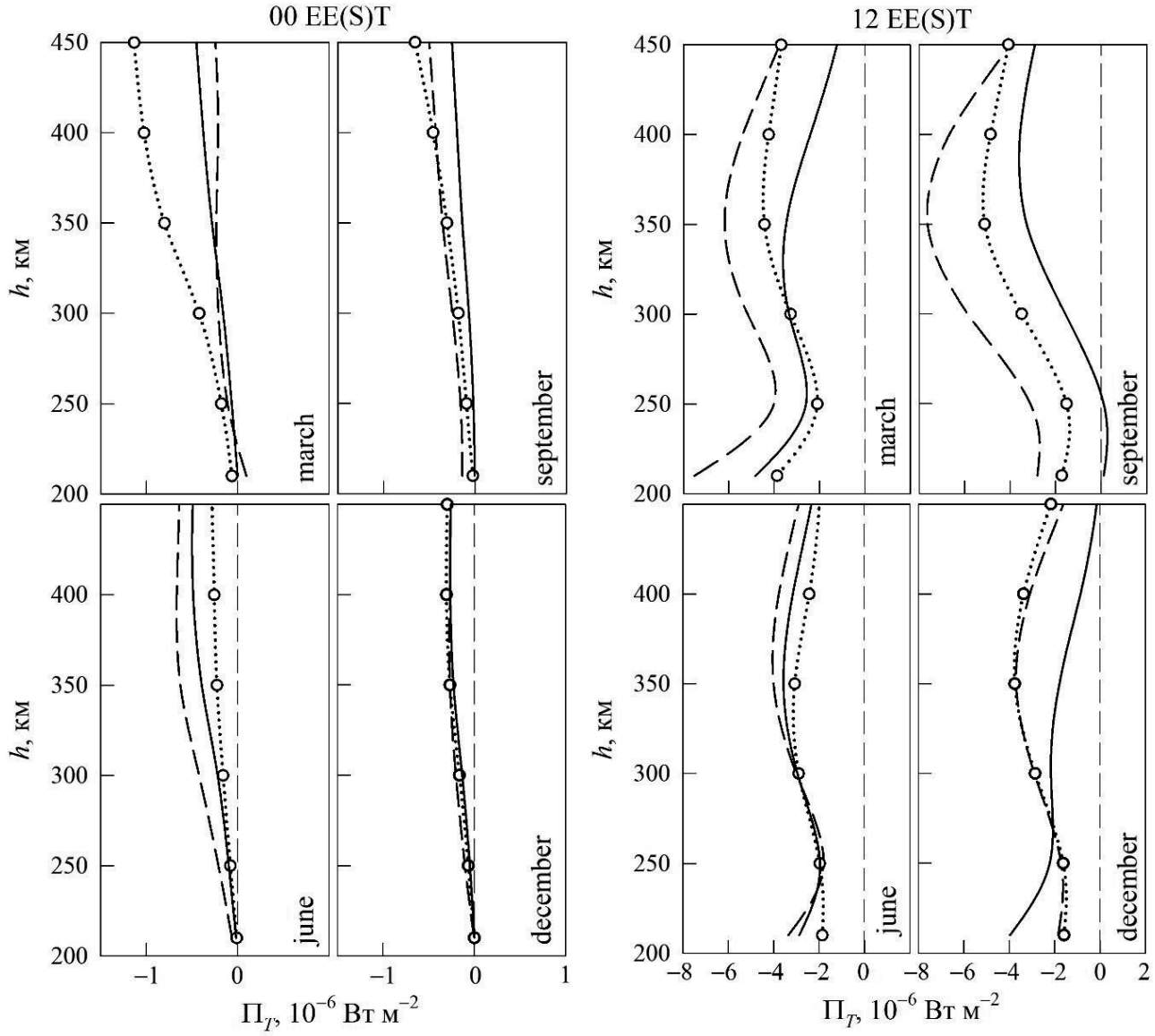

Fig. 4. Altitude profiles of the heat flux density transferred by electrons to the ionosphere from the plasmasphere in the typical geophysical periods during 2017–2019 for 00 (left panel) and 12 EE(S)T (right panel)

6. Conclusions

In this paper, we simulate variations in the parameters of thermal processes in the ionospheric plasma for periods close to the periods of summer and winter solstices, vernal and autumn equinoxes in 2017–2019.

The analysis of spatial-temporal and seasonal variations of parameters of thermal processes in the ionosphere on the phase of decline/minimum of the 24th cycle of solar activity is presented. The values of the energy supplied to the electron gas and the heat flux density transferred by electrons from the plasmasphere to the ionosphere are calculated. The obtained quantitative characteristics of the parameters, the shape of their height profiles and diurnal variations are typical for the considered seasons.

The obtained simulation results can be used in basic research of solar-terrestrial relations and geospace, for further development of the CERIM IION regional ionosphere model, as well as for solving applied problems related to the possibility of space weather predicting.

References

1. Lyashenko, M.V., Sklyarov, I.B., Chernogor, L.F. (2006). Diurnal and seasonal variations of ionospheric plasma parameters during the period of solar activity decline. *Space Science and Technology, 12*(2/3), 45–58.

2. Lyashenko, M.V., Chernogor, L.F., Chernyak, Yu.V. (2006). Diurnal and seasonal variations in the parameters of the ionospheric plasma during the maximum solar activity. *Space Science and Technology, 12*(4), 56–70.

3. Lyashenko, M.V., Pulyaev, V.A., Chernogor, L.F. (2006). Diurnal and seasonal variations in the parameters of the ionospheric plasma during the growth of solar activity. *Space science and technology*, *12*,(5/6), 58–68.

4. Dzyubanov, D.A., Lyashenko, M.V., Chernogor, L.F. (2008). Research and modeling of variations in ionospheric plasma parameters during the minimum period of the 23rd solar activity cycle. *Space Science and Technology*, *14*(1), 44–56.

5. Domnin, I.F., Chepurnyy, Ya.M., Emelyanov, L.Ya., Chernyaev, S.V., Kononenko, A.F., Kotov, D.V., … Iskra, D.A. (2014). Kharkiv incoherent scatter facility. *Bulletin of NTU "KhPI". Series: Radiophysics and ionosphere*, *47*(1089), 28–42.

6. Chernogor, L., Domnin, I., Lyashenko, M. (2010). Development of Central Europe Regional Ionospheric Model (CERIM IION) for Space Weather Forecasting. *EGU General Assembly 2010*. Proceedings of the Conference. Vienna, Austria.

7. Iskra, D.A., Kolodyazhnyi, V.V., Lyashenko, M.V. (2019). Development of the CERIM IION regional ionosphere model as part of the creation of the space weather forecast service. *Theoretical and applied aspects of radio engineering, instrument making and computer technologies*, Proceedings of the IV International Scientific and Technical Conference. Ternopil, Ukraine.

8. Picone, J.M., Hedin, A.E., Drob, D.P. (2002). NRLMSISE-00 empirical model of the atmosphere: Statistical comparisons and scientific issues. *Journal of Geophysical Research*, *107*(A12), 1–16.

9. Yemelyanov, L.Ya. (2017). Development of principles and instrumentation for generation of test and control signals of the incoherent scatter radar. *Telecommunications and Radio Engineering*, *76*(14), 1259–1271. doi: 10.1615/TelecomRadEng.v76.i14.50.

10. Schunk, R.W., Nagy A.F. (2009). *Ionospheres: Physics, Plasma Physics, and Chemistry*. Cambridge University Press.